STRESS WAVE PROPAGATION IN RECTANGULAR BARS

W. B. FRASER

Department of Applied Mathematics, The University of Sydney, Australia

Abstract—The method of collocation is used to obtain dispersion curves for wave propagation in infinite rectangular bars. It is found to give accurate results, over a limited range of wave numbers, for the first two branches of the dispersion curves for the various modes of propagation. For the square bar the screw modes of Kynch are found and the interaction between one of the screw modes and the longitudinal mode is investigated in detail. Finally, these results are used to assess the accuracy of two recent approximate theories for waves in bars.

NOTATION

a	semiwidth of rectangular section
b	semidepth of rectangular section
c	phase velocity
c_1	$= [(\lambda + 2\mu)/\rho]^{\frac{1}{2}}$ velocity of dilational waves in an infinite medium
c_2	$= (\mu/\rho)^{\frac{1}{2}}$ velocity of shear waves in an infinite medium
c_0	$= (E/\rho)^{\frac{1}{2}} = c_2[2(1+v)]^{\frac{1}{2}}$ the bar velocity
c_s	Rayleigh wave velocity
E	Young's Modulus
$A_n, \dots, F_n$	constant coefficients in series solutions
i	$= \sqrt{(-1)}$
$J_n(s)$	Bessel's function of order n
$J_n'(s)$	$= dJ_n/ds$
$js_n(\alpha)$	$= J_n(\alpha r)\sin n\theta$
$js_n(\beta)$	$= J_n(\beta r)\sin n\theta$
$jc_n(\alpha)$	$= J_n(\alpha r)\cos n\theta$
$jc_n(\beta)$	$= J_n(\beta r)\cos n\theta$
k	$= \omega/c$ wave number
K	$= \frac{1}{2}(\beta^2 - k^2)/\alpha^2$ *
t	time
r, θ, z	cylindrical polar coordinates
x, y, z	cartesian coordinates
u_r, u_θ, u_z	cylindrical polar components of displacement
u_x, u_y, u_z	cartesian components of displacement
α	$= k(c^2/c_1^2 - 1)^{\frac{1}{2}}$ *
β	$= k(c^2/c_2^2 - 1)^{\frac{1}{2}}$
λ, μ	Lamé's constants
v	Poisson's ratio
ρ	density
$\sigma_{rr}, \sigma_{r\theta}, \dots, \sigma_{zz}$	cylindrical polar components of stress
$\sigma_{xx}, \sigma_{xy}, \dots, \sigma_{zz}$	cartesian components of stress
σ_{max}	maximum stress (amplitude) in the bar
ω	$= 2\pi \times$ frequency

Note on the use of terms mode and branch

In this paper *mode* refers to the broad classification of the types of wave that propagate in rectangular bars, and *branch* refers to a particular dispersion curve in the family of dispersion curves belonging to a given *mode*.

* In section 6, K and α are the adjustment parameters of Volterra and Medick respectively.

Thus, the following letters are used to designate the various *modes* of wave propagation:

L longitudinal mode
T torsional mode
S_1 first screw mode
S_2 second screw mode
B_x bending mode (about the x-axis)
B_y bending mode (about the y-axis)

and when a particular *branch* is referred to a superscript will be added to the letter. For example T^1 designates the first (or fundamental) *branch* of the torsional *mode*.

1. INTRODUCTION

AN EXACT solution to the problem of elastic wave propagation in infinite bars is only possible for bars of circular cross-section. For bars of noncircular cross-section a number of approximate methods for finding dispersion relations have been developed, and a review of these (up to 1960) is given by Green [1]. More recently Volterra [12] and Medick [13, 14] have put forward approximate theories that are particularly appropriate for bars of rectangular cross-section, and the results obtained in this paper will be used to assess the accuracy of these two theories.

Here the method of collocation is used to obtain dispersion curves for waves in rectangular bars. Exact solutions of the elastic wave equations in cylindrical polar coordinates are made to satisfy the boundary conditions at a discrete set of points on the boundary. This gives rise to a determinant, the zeros of which give points on the dispersion curves. The first (and in some cases the second) branches of the dispersion curves for all modes of wave propagation in square bars, and some rectangular bars, have been obtained in this way. The method is unsatisfactory for obtaining the higher order branches, or the low order branches at high frequencies; it is also unsatisfactory when the ratio of the lengths of the sides of the section is large.

The results of three previous investigations are especially relevant to the present work. Kynch [2] used the variational method to find approximate dispersion relations for noncircular bars. He found that four modes of wave propagation are possible in a rectangular bar: longitudinal, torsional and two bending modes. In a square bar he found that owing to the additional symmetry of the cross-section two additional modes, which he called screw modes, are possible; the longitudinal mode separates into a symmetrical longitudinal and a screw mode, and the torsional mode separates into a torsional and a second screw mode. On the basis of these results Kynch explained the experimental results of Morse [3] for longitudinal waves in rectangular brass bars. Recently, Nigro [4] used the variational method to obtain more accurate dispersion curves for rectangular bars. Unfortunately, he failed to distinguish the screw from the longitudinal and torsional modes in the square bar and his results must be reinterpreted. The collocation method leads us naturally to the modes of wave propagation identified by Kynch, and dispersion curves similar to the experimental curves of Morse are obtained. For the square bar our results are in excellent agreement with those of Nigro (when the latter are reinterpreted).

This appears to be the first work in which collocation is used to obtain dispersion curves. However, finding dispersion curves is essentially an eigenvalue problem and collocation has been used previously by Fox, Henrici and Moler [5] to find the eigen-frequencies of an L shaped membrane and by Conway and Leissa [6] and Conway and Farnham [7] to solve problems of the buckling and vibration of plates. Although results are given here only for

rectangular bars, the method can be applied to bars with other cross-sections such as convex polygons and ellipses where the ratio of the major to the minor axis is not too large.

2. THE COLLOCATION METHOD

We take the general solutions of the elastic wave equations in cylindrical polar coordinates (r, θ, z) given by Kynch and Green [8]. The components of displacement (u_r, u_θ, u_z) in the radial, transverse, and axial directions respectively are

$$u_r = \frac{1}{4\mu} \sum_{n=0}^{\infty} \{A_n n J_n(\beta r)/\beta^2 r + B_n J'_n(\beta r)/\beta + C_n J'_n(\alpha r)/\alpha\} \cos n\theta \exp[i(kz - \omega t)]$$

$$+ \frac{1}{4\mu} \sum_{n=0}^{\infty} \{D_n, E_n, F_n\} \sin n\theta \exp[i(kz - \omega t)],$$

$$u_\theta = -\frac{1}{4\mu} \sum_{n=0}^{\infty} \{A_n J'_n(\beta r)/\beta + B_n n J_n(\beta r)/\beta^2 r + C_n n J_n(\alpha r)/\alpha^2 r\} \sin n\theta \exp[i(kz - \omega t)]$$

$$+ \frac{1}{4\mu} \sum_{n=0}^{\infty} \{D_n, E_n, F_n\} \cos n\theta \exp[i(kz - \omega t)],$$

$$u_z = \frac{1}{4\mu} \sum_{n=0}^{\infty} \{-B_n i J_n(\beta r)/k + C_n ik J_n(\alpha r)/\alpha^2\} \cos n\theta \exp[i(kz - \omega t)]$$

$$+ \frac{1}{4\mu} \sum_{n=0}^{\infty} \{E_n, F_n\} \sin n\theta \exp[i(kz - \omega t)]. \tag{1}$$

The notation $\{D_n, E_n, F_n\}$ is used to indicate that this expression is the same as that in the immediately preceding braces with $D_n, E_n,$ and F_n, replacing A_n, B_n and C_n respectively. In subsequent equations the factor $\exp[i(kz - \omega t)]$ will be omitted. The components of stress are

$$\sigma_{rr} = \sum_{n=0}^{\infty} \{A_n \tfrac{1}{2} n[\beta r J'_n(\beta r) - J_n(\beta r)]/(\beta r)^2 + B_n \tfrac{1}{2} J''_n(\beta r) + C_n \tfrac{1}{2} [J''_n(\alpha r) - (K-1)J_n(\alpha r)]\} \cos n\theta$$

$$+ \sum_{n=0}^{\infty} \{D_n, E_n, F_n\} \sin n\theta,$$

$$\sigma_{r\theta} = \sum_{n=0}^{\infty} \{A_n \tfrac{1}{2} [\beta r J'_n(\beta r) + (\tfrac{1}{2}\beta^2 r^2 - n^2)J_n(\beta r)]/(\beta r)^2 - B_n \tfrac{1}{2} n[\beta r J'_n(\beta r) - J_n(\beta r)]/(\beta r)^2$$

$$- C_n \tfrac{1}{2} n[\alpha r J'_n(\alpha r) - J_n(\alpha r)]/(\alpha r)^2\} \sin n\theta - \sum_{n=0}^{\infty} \{D_n, E_n, F_n\} \cos n\theta,$$

$$\sigma_{rz} = \sum_{n=0}^{\infty} \{A_n \tfrac{1}{4} ikn J_n(\beta r)/\beta^2 r - B_n \tfrac{1}{4} i(\beta^2 - k^2)J'_n(\beta r)/k\beta$$

$$+ C_n \tfrac{1}{2} ik J'_n(\alpha r)/\alpha\} \cos n\theta + \sum_{n=0}^{\infty} \{D_n, E_n, F_n\} \sin n\theta,$$

$$\sigma_{\theta\theta} = \sum_{n=0}^{\infty} \{ -A_n \tfrac{1}{2} n[\beta r J_n'(\beta r) - J_n(\beta r)]/(\beta r)^2 + B_n \tfrac{1}{2} [\beta r J_n'(\beta r) - n^2 J_n(\beta r)]/(\beta r)^2$$

$$- C_n \tfrac{1}{2} [J_n''(\alpha r) + K J_n(\alpha r)]\} \cos n\theta + \sum_{n=0}^{\infty} \{ D_n, E_n, F_n \} \sin n\theta,$$

$$\sigma_{\theta z} = \sum_{n=0}^{\infty} \{ -A_n \tfrac{1}{4} ik J_n'(\beta r)/\beta + B_n \tfrac{1}{4} i(\beta^2 - k^2) n J_n(\beta r)/k\beta^2 r$$

$$- C_n \tfrac{1}{2} ikn J_n(\alpha r)/\alpha^2 r \} \sin n\theta - \sum_{n=0}^{\infty} \{ D_n, E_n, F_n \} \cos n\theta,$$

$$\sigma_{zz} = \sum_{n=0}^{\infty} \tfrac{1}{2} \{ B_n J_n(\beta r) - C_n[K - 1 + (k/\alpha)^2] J_n(\alpha r) \} \cos n\theta + \sum_{n=0}^{\infty} \tfrac{1}{2} \{ E_n, F_n \} \sin n\theta, \qquad (2)$$

where $K = \tfrac{1}{2}(\beta^2 - k^2)/\alpha^2$.

In the case of a circular bar, with its axis coinciding with the z-axis, the boundary conditions

$$\sigma_{rr} = \sigma_{r\theta} = \sigma_{rz} = 0 \quad \text{at} \quad r = R$$

(where R is the radius of the bar) are satisfied by the above solutions for each value of n separately. When $n = 0$, the solutions involving the coefficients B_0 and C_0 represent longitudinal waves, and those involving D_0 represent torsional waves. When $n > 0$ the boundary conditions are satisfied by solutions involving either the coefficients A_n, B_n, and C_n, or the coefficients D_n, E_n, and F_n; one set of solutions being obtained from the other by rotating the axes π/n radians about the z-axis.

For noncircular bars the stresses and displacements are still given by equations (1) and (2), and in general we must now retain all the terms in the infinite series to satisfy the boundary conditions. In order to impose the boundary conditions we require the normal and tangential components of stress on the boundary, and for a rectangular bar these are simply cartesian components. Transforming (1) and (2) we find that the cartesian components of displacement are

$$u_x = \frac{1}{\mu} \sum_{n=0}^{\infty} \{ A_n[jc_{n+1}(\beta) + jc_{n-1}(\beta)]/\beta + B_n[-jc_{n+1}(\beta) + jc_{n-1}(\beta)]/\beta$$

$$+ c_n[-jc_{n+1}(\alpha) + jc_{n-1}(\alpha)]/\alpha \} + \frac{1}{\mu} \sum_{n=0}^{\infty} \{ D_n, E_n, F_n, js \},$$

$$u_y = \frac{1}{\mu} \sum_{n=0}^{\infty} \{ A_n[js_{n+1}(\beta) - js_{n-1}(\beta)]/\beta - B_n[js_{n+1}(\beta) + js_{n-1}(\beta)]/\beta$$

$$- c_n[js_{n+1}(\alpha) + js_{n-1}(\alpha)]/\alpha \} - \frac{1}{\mu} \sum_{n=0}^{\infty} \{ D_n, E_n, F_n, jc \},$$

$$u_z = \frac{2}{\mu} \sum_{n=0}^{\infty} \{ -B_n ijc_n(\beta)/k + C_n ikjc_n(\alpha)/\alpha^2 \} + \frac{2}{\mu} \sum_{n=0}^{\infty} \{ E_n, F_n, js \}, \qquad (3)$$

and the cartesian components of stress are

$$\sigma_{xx} = \sum_{n=0}^{\infty} \{A_n[-jc_{n+2}(\beta)+jc_{n-2}(\beta)] + B_n[jc_{n+2}(\beta)+jc_{n-2}(\beta)-2jc_n(\beta)]$$

$$+ C_n[jc_{n+2}(\alpha)+jc_{n-2}(\alpha)-2(2K-1)jc_n(\alpha)]\} + \sum_{n=0}^{\infty} \{D_n, E_n, F_n, js\},$$

$$\sigma_{xy} = \sum_{n=0}^{\infty} \{A_n[js_{n+2}(\beta)-js_{n-2}(\beta)] + B_n[js_{n+2}(\beta)-js_{n-2}(\beta)]$$

$$+ C_n[js_{n+2}(\alpha)-js_{n-2}(\alpha)] - \sum_{n=0}^{\infty} \{D_n, E_n, F_n, jc\},$$

$$\sigma_{xz} = \sum_{n=0}^{\infty} \{A_n[jc_{n+1}(\beta)+jc_{n-1}(\beta)]ik/\beta + B_n[jc_{n+1}(\beta)-jc_{n-1}(\beta)]i(\beta^2-k^2)/\beta k$$

$$+ C_n[-jc_{n+1}(\alpha)+jc_{n-1}(\alpha)]2ik/\alpha\} + \sum_{n=0}^{\infty} \{D_n, E_n, F_n, js\},$$

$$\sigma_{yy} = \sum_{n=0}^{\infty} \{A_n[jc_{n+2}(\beta)-jc_{n-2}(\beta)] - B_n[jc_{n+2}(\beta)+jc_{n-2}(\beta)+2jc_n(\beta)]$$

$$- C_n[jc_{n+2}(\alpha)+jc_{n-2}(\alpha)+2(2K-1)jc_n(\alpha)]\} + \sum_{n=0}^{\infty} \{D_n, E_n, F_n, js\},$$

$$\sigma_{yz} = \sum_{n=0}^{\infty} \{A_n[js_{n+1}(\beta)+js_{n-1}(\beta)]ik/\beta + B_n[js_{n+1}(\beta)+js_{n-1}(\beta)]i(\beta^2-k^2)/\beta k$$

$$- C_n[js_{n+1}(\alpha)+js_{n-1}(\alpha)]2ik/\alpha\} - \sum_{n=0}^{\infty} \{D_n, E_n, F_n, jc\},$$

$$\sigma_{zz} = \sum_{n=0}^{\infty} 4\{B_n jc_n(\beta) - C_n[K-1+(k/\alpha)^2]jc_n(\alpha)\} + \sum_{n=0}^{\infty} 4\{E_n, F_n, js\}, \tag{4}$$

where

$$js_n(\alpha) = J_n(\alpha r)\sin n\theta, \qquad js_n(\beta) = J_n(\beta r)\sin n\theta.$$

$$jc_n(\alpha) = J_n(\alpha r)\cos n\theta, \qquad jc_n(\beta) = J_n(\beta r)\cos n\theta.$$

In equations (3) and (4) in addition to the convention adopted in (1) and (2) the occurrence of jc in the braces means that everywhere js occurs in the preceding braces it is to be replaced by jc, and vice versa. Note that the coefficients $A_n, \ldots, F_n$ occurring in (3) and (4) are one-eighth of the corresponding coefficients in (1) and (2).

For an infinite rectangular bar with its axis coinciding with the z-axis and its boundaries formed by the planes $x = \pm a$, $y = \pm b$, (see figure 1) the solutions (3) and (4) represent harmonic waves travelling along the z-axis provided they can be made to satisfy the boundary conditions

$$\sigma_{xx} = \sigma_{xy} = \sigma_{xz} = 0 \quad \text{on} \quad x = \pm a, \qquad (r = a\sec\theta),$$

$$\sigma_{yy} = \sigma_{yx} = \sigma_{yz} = 0 \quad \text{on} \quad y = \pm b, \qquad (r = b\csc\theta).$$
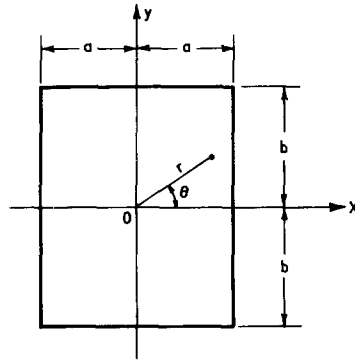
Fig. 1. Coordinate system for a rectangular cross-section.

These boundary conditions can be satisfied approximately if we make the stresses zero at a discrete set of points on the boundary (called collocation points).

For bars with at least one axial plane of symmetry the series (3) and (4) separate into two sets of solutions; one involves only the terms with coefficients A_n, B_n and C_n, the other involves the terms with coefficients D_n, E_n and F_n. Suppose we retain N terms in one of these solutions, then the truncated series involve $3N$ arbitrary coefficients. If we also chose N collocation points, and set each of the three truncated series representing the normal and tangential components of stress at each point equal to zero, we obtain $3N$ homogeneous, linear equations for the $3N$ unknown coefficients. This set of equations has a nontrivial solution if and only if its determinant is equal to zero. We will call this determinant the collocation determinant.

If the ratio of the side lengths of the cross-section and the value of Poisson's ratio are given then the elements of the collocation determinant depend only on the parameters c/c_2 and ka. The real values of c/c_2 and ka for which the determinant is zero give the phase velocity and frequency of waves that propagate along the bar without attenuation. Before discussing the numerical procedure and results we examine the collocation determinant in more detail.

3. CONSTRUCTION OF THE COLLOCATION DETERMINANT FOR EACH MODE

(a) *Rectangular bar*

Because of the twofold symmetry of the rectangular cross-section, the solutions (3) and (4) separate into four infinite series each of which is capable of satisfying the boundary conditions. The four solutions correspond to the four modes of wave propagation in a rectangular bar.

(i) *Longitudinal* (L) *mode.* We obtain the solution that represents longitudinal waves by considering the series of terms involving the coefficients A_n, B_n, and C_n with n even. This solution gives displacements and stresses that are symmetrical with respect to both the x- and the y-axis. Thus for the displacements we have

$$u_x(-\theta, r) = u_x(\theta, r) = -u_x(\pi - \theta, r),$$

$$-u_y(-\theta, r) = u_y(\theta, r) = u_y(\pi - \theta, r),$$

$$u_z(-\theta, r) = u_z(\theta, r) = u_z(\pi - \theta, r), \tag{5a}$$

and for the stresses we have

$$\sigma_{xx}(-\theta, r) = \sigma_{xx}(\theta, r) = \sigma_{xx}(\pi - \theta, r),$$

$$-\sigma_{xy}(-\theta, r) = \sigma_{xy}(\theta, r) = -\sigma_{xy}(\pi - \theta, r),$$

$$\sigma_{xz}(-\theta, r) = \sigma_{xz}(\theta, r) = -\sigma_{xz}(\pi - \theta, r),$$

$$\sigma_{yy}(-\theta, r) = \sigma_{yy}(\theta, r) = \sigma_{yy}(\pi - \theta, r),$$

$$-\sigma_{yz}(-\theta, r) = \sigma_{yz}(\theta, r) = \sigma_{yz}(\pi - \theta, r),$$

$$\sigma_{zz}(-\theta, r) = \sigma_{zz}(\theta, r) = \sigma_{zz}(\pi - \theta, r). \tag{5b}$$

If we satisfy the boundary conditions on a quarter of the boundary (say that part of the boundary in the positive quadrant of the xy-plane) then equations (5b) insure us that the boundary conditions are satisfied on the rest of the boundary. Thus it is only necessary to choose collocation points on one quarter of the boundary. (This is also true for the other three modes.)

Since the terms involving the coefficients A_0 are all identically zero the first column of the collocation determinant is zero. We overcome this difficulty by choosing the intersection of the boundary and the x-axis (or the y-axis), where $\sigma_{xy} \equiv 0$, as a collocation point. This introduces a zero row into the determinant and if the zero row and column are deleted the reduced collocation determinant is nontrivial.

(ii) *Torsional* (T) *mode.* For the series of terms involving D_n, E_n and F_n with n even, the symmetry relations are obtained by reversing the signs on the first and third terms in equations (5). These stresses and displacements are asymmetrical with respect to the x- and y-axis, and correspond to a shearing deformation of the bar. This solution represents waves propagating in the torsional mode.

Since all the terms involving the coefficients E_0 and F_0 are zero, this collocation determinant has two zero columns. By choosing one of the collocation points at the intersection of the boundary with the x-axis (or the y-axis), where $\sigma_{xx} \equiv 0$ and $\sigma_{xz} \equiv 0$, we introduce two zero rows into the determinant, which when deleted with the zero columns gives a nontrivial reduced determinant.

(iii) *Bending* (B) *modes.* Similarly, the series of terms involving the coefficients A_n, B_n, and C_n with n odd, give stresses and displacements that are symmetrical about the x-axis and asymmetrical about the y-axis, and the series involving D_n, E_n, and F_n, with n odd, give stresses and displacements that are asymmetrical about the x-axis and symmetrical about the y-axis. These solutions represent waves propagating in modes of bending about the y-axis and the x-axis respectively (designated the B_y and B_x modes).

The collocation determinants for these cases have no identically zero columns, and collocation points that would lead to identically zero rows must be avoided.

(b) *Square bar*

A square bar has four axial planes of symmetry and the even series that gave the longitudinal and torsional modes for the rectangular bar separate to give four solutions: longitudinal, torsional, and two screw modes. The odd series do not separate further, but again give the two bending modes. Figure 2 shows, schematically, the distortion of the cross-section for the six modes of wave propagation in a square bar.
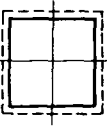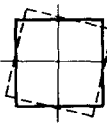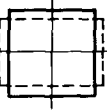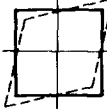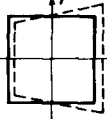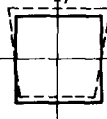
	Terms involving A_n, B_n, C_n.	Terms involving D_n, E_n, F_n.
n = 0, 4, 8, ⋯	L mode: Longitudinal waves	T mode: Torsional waves
n = 2, 6, 10, ⋯	S_1 mode: Screw waves relative to x, y axis	S_2 mode: Screw waves relative to diagonals
n = 1, 3, 5, ⋯	B_y mode: Bending waves relative to y-axis	B_x mode: Bending waves relative to x-axis

FIG. 2. Summary of the modes of vibration of a square bar and the corresponding terms in the series solutions.

(i) *Longitudinal* (L) *and first screw* (S_1) *mode.* Consider the series of terms involving A_n, B_n, and C_n, with $n = 0, 4, 8, \ldots$. As well as the symmetry relations (5) we have the following symmetry relations with respect to the diagonals of the cross-section:

With respect to the diagonal $x = y$,

$$u_x(\pi/2 - \theta, r) = u_y(\theta, r),$$
$$u_z(\pi/2 - \theta, r) = u_z(\theta, r), \tag{6a}$$

and

$$\sigma_{xx}(\pi/2 - \theta, r) = \sigma_{yy}(\theta, r),$$
$$\sigma_{xy}(\pi/2 - \theta, r) = \sigma_{yx}(\theta, r),$$
$$\sigma_{xz}(\pi/2 - \theta, r) = \sigma_{yz}(\theta, r),$$
$$\sigma_{zz}(\pi/2 - \theta, r) = \sigma_{zz}(\theta, r), \tag{6b}$$

and similar relations with respect to the diagonal $x = -y$. Equations (5) and (6), taken together, show that the stresses and displacements are symmetrical with respect to all four planes of symmetry and this solution, therefore, represents longitudinal waves. If, now, we satisfy the boundary conditions on one eighth of the boundary (say $x = a$, $0 \leq y \leq b$) equations (5) and (6) insure us that they are satisfied on the rest of the boundary.

For the series of terms involving A_n, B_n, and C_n, with $n = 2, 6, 10, \ldots$, the symmetry relations with respect to the diagonals are obtained by reversing the signs on the right hand sides of equations (6). When these relations are considered with equations (5) we see that the stresses and displacements are symmetrical with respect to the x- and y-axes and asymmetrical with respect to the diagonals. This solution corresponds to a deformation in which the bar is squeezed alternately in the direction of the x- and then the y-axis, and is the first screw mode. Again it is only necessary to satisfy the boundary conditions on one eighth of the boundary. (This is also true for the torsional and second screw mode.)

(ii) *Torsional* (T) *and second screw* (S_2) *modes.* The series involving D_n, E_n, and F_n, with $n = 0, 4, 8, \ldots$, give stresses and displacements which are asymmetrical with respect to all four planes of symmetry, while the series involving D_n, E_n, and F_n, with $n = 2, 6, 10, \ldots$, give stresses and displacements which are asymmetrical with respect to the x- and y-axes, and symmetrical with respect to the diagonals. The first of these solutions corresponds to a deformation in which the cross-section undergoes a net rotational oscillation, and is therefore the torsional mode; the second corresponds to a deformation in which the bar is squeezed alternately in the direction of one diagonal and then the other, and is the second screw mode.

(iii) *Bending* (B) *mode.* The collocation determinants for the bending modes in a square bar are the same as those for the rectangular bar and collocation points must still be chosen on one quarter of the boundary. However for a square bar the dispersion curves for the B_x and B_y modes are indistinguishable, and these modes will simply be referred to as the B mode of wave propagation.

4. NUMERICAL PROCEDURE AND ACCURACY

As stated in Section 2, once the values of Poisson's ratio (v) and the ratio of the side lengths of the cross-section (b/a) are fixed the value of the collocation determinant depends only on ka and c/c_2. The results given here are all for $v = 0.3$ with values of b/a ranging from 1 to 2.

For a particular value of ka and a given number of equally spaced collocation points, the value of c/c_2 that makes the determinant zero is calculated by iteration. (For the square bar the initial values of c/c_2 used to start the iteration were taken from Nigro's results [4].) This procedure is repeated for increasing numbers of collocation points until successive values of c/c_2 are in agreement to a suitable number of decimal places. The ratios of the coefficients (A_n, B_n, C_n, or D_n, E_n, F_n, as the case may be) are now calculated, and from these the stresses and displacements (normalized with respect to the maximum stress and displacement) at any point in the cross-section can be found. In particular, the stresses at points on the boundary midway between the collocation points are calculated, and their nearness to zero provides a further indication of the accuracy of the result.

(a) *Square bar*

Table 1 gives the numerical results for the first branches of the six modes of propagation in a square bar. For $0 < ka \leq 5$ eight collocation points (on one-eighth of the boundary) are found to give c/c_2 accurate to four decimal places for the L^1, S_1^1, T^1, and S_2^1 branches, and the stresses between the collocation points are in most cases less than $\sigma_{max} \times 10^{-4}$, where σ_{max} is the maximum stress in the bar. In fact, four collocation points give c/c_2 accurate to three decimal places, although some of the stresses at the intermediate points are now as large as $\sigma_{max} \times 10^{-2}$. Sixteen collocation points (on one quarter of the boundary) are necessary to obtain the same accuracy for the B^1 branch. On the second branches of these modes, for the same range of ka, the same number of, collocation points give c/c_2 accurate to three decimal places. For larger values of ka, and higher order branches the accuracy falls off rapidly unless a very large number of collocation points is used.

The reason for these limitations on the accuracy of the method is readily found. For points on the L^1 branch with low values of ka the arguments of the Bessel functions in

TABLE 1. PHASE VELOCITY c/c_2 AS A FUNCTION OF ka FOR THE FUNDAMENTAL BRANCHES OF THE DISPERSION CURVES FOR A SQUARE BAR WITH $v = 0.3$

ka	c/c_2				
	L^1	S_1^1	T^1	S_2^1	B_x^1 & B_y^1
0·10	1·6120				0·0925
0·30	1·6080				0·2643
0·50	1·5996		0·9183	3·840	0·4058
0·75	1·5814			2·567	0·5382
1·00	1·5512	2·1646	0·9182	1·9680	0·6316
1·20	1·5150	1·8074	0·9179	1·6902	0·6864
1·40	1·4657	1·5640	0·9177	1·5066	0·7286
1·60	1·4048	1·3926	0·9175	1·3802	0·7614
1·80	1·3385	1·2694	0·9172	1·2902	0·7874
2·00	1·2743	1·1793	0·9169	1·2246	0·8081
2·20	1·2172	1·1127	0·9167	1·1754	0·8249
2·40	1·1687	1·0631	0·9163	1·1380	0·8385
2·60	1·1285	1·0258	0·9160	1·1089	0·8497
2·80	1·0956		0·9156	1·0861	0·8592
3·00	1·0688	0·9759		1·0677	0·8664
3·20		0·9594		1·0528	0·8731
3·40	1·029	0·9467		1·0406	0·8781
3·60		0·9368		1·0304	0·8830
3·80		0·9292			0·8868
4·00	0·992	0·9232	0·913		0·8893
5·00	0·962	0·908		0·990	0·899
6·00	0·948	0·904	0·909	0·977	0·902
7·00	0·942	0·903		0·968	0·903
8·00	0·938	0·903	0·907	0·961	0·903
9·00	0·936	0·903		0·956	
10·00	0·934	0·903	0·905	0·952	
12·00	0·932		0·905	0·946	
14·00	0·931		0·905	0·942	
16·00	0·931			0·940	

equation (3) and (4) (taking the terms containing A_n, B_n, C_n with $n = 0, 4, 8, \ldots$) are very small and with increasing n, $J_n \to 0$, so that the first few terms in the series give a good representation of the actual stress and displacement distributions (which are fairly simple). When ka is large, the arguments of the Bessel functions are large and J_n does not decrease so rapidly with increasing n; the stress and displacement distributions are more complicated and more terms must be retained in the series to give a good approximation. A similar argument applies for the higher order branches, and for the other modes.

(b) *Rectangular bar*

Sixteen collocation points equally spaced on one-quarter of the boundary of the rectangular bar for which $b/a = 1.2$ give results with the same accuracy as those discussed above for the square bar. When $b/a = 2$, using the same spacing of collocation points, we can calculate c/c_2 accurate to two decimal places for the first two branches and $0 < ka \leq 5$. As b/a increases it is no longer appropriate to use the solutions (3) and (4) in cylindrical polar coordinates with the collocation method. An investigation to find a more appropriate solution of the elastic wave equations to use with the collocation method for these cases is beyond the scope of the present work.

5. RESULTS AND DISCUSSION

Although some results are obtained for all modes of wave propagation in rectangular bars, most attention is given to the L and S_1 modes. As suggested by Kynch [2] the equivoluminal waves of Lamé [9], which propagate with phase velocity $c = c_2\sqrt{2}$ at wave numbers given by $ka = n\pi/2$ (n odd) for bars of width $2a$, play an important role in classifying and comparing the branches of the dispersion curves for the L modes of various bars. Mindlin and Fox [10] also found exact solutions of the elastic wave equations for certain waves in rectangular bars with certain ratios of width to depth. Their solutions give a discrete set of points on the dispersion curves, but except for the Lamé waves (which are included in their solutions) these points appear to lie on higher order branches than those obtained here.

(a) *Longitudinal and first screw modes*

(i) *Square bar.* Figure 3 shows the first two branches of the dispersion curves for the L and S_1 modes. The L^1 and S_1^1 branches intersect, and at this value of ka waves given by linear combinations of the L and S_1 mode solutions are possible. If we add two such solutions of equal amplitude we can see from their symmetry relations that the S_1 mode
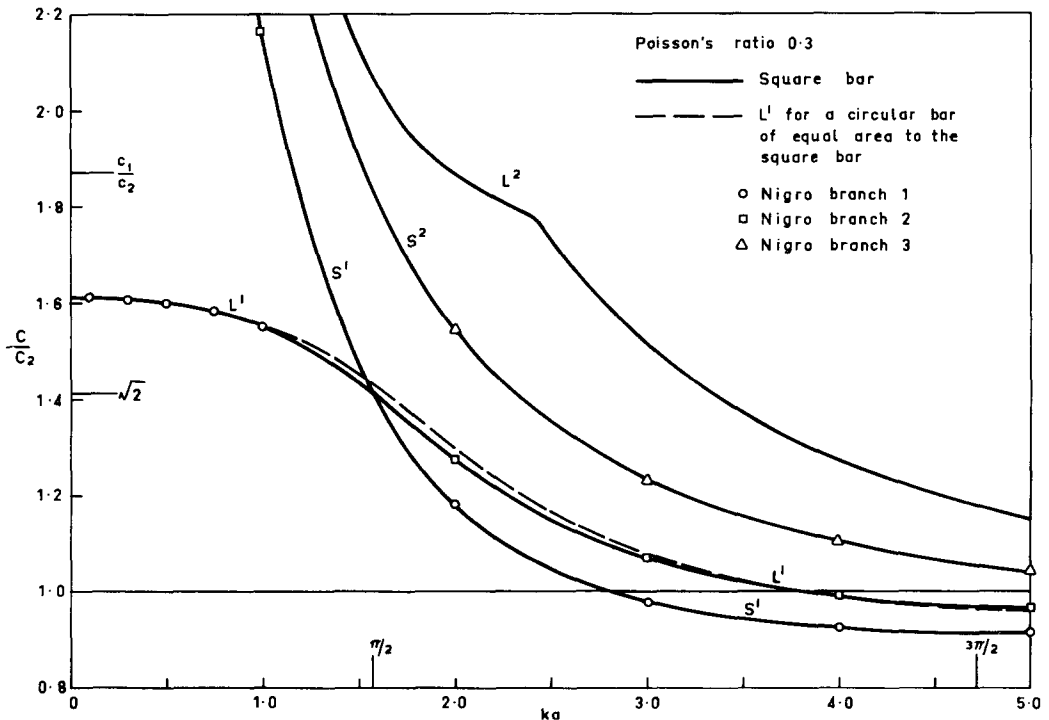

FIG. 3. Dispersion curves for a square bar: branches L^1, L^2, S_1^1, and S_1^2.

reinforces the stresses and displacements of the L mode on planes parallel to the yz-plane (or the xz-plane) and exactly cancels them on planes parallel to the xz-plane (or the

yz-plane). This combination solution, where stresses and displacements on planes parallel to the xz-plane (or the yz-plane) are zero, corresponds to one of Lamé's equivoluminal waves and branches L^1 and S_1^1 therefore intersect at $ka = \pi/2$. Although the branches L^2 and S_1^2 do not intersect, some of the higher branches will intersect at $ka = n\pi/2$, $n = 3, 5, \ldots$. Because of the limitations of the collocation method discussed in the last section these higher branches have not been obtained.

Using the simplest approximate displacements in conjunction with the variational principle Kynch [2] found the two screw modes as well as the longitudinal and torsional modes for square bars, and showed that the L^1 and S_1^1 branches intersect. Nigro [4] used more comprehensive approximate displacements to obtain more accurate dispersion curves for rectangular bars. The power series he used to represent the longitudinal and torsional modes in rectangular bars also represent the screw modes for the square bar if the sign of every second term is reversed. Thus, using these series for the square bar, Nigro has identified all his results as either L or T modes, whereas some of them are actually S_1 and S_2 modes respectively. The results that he has identified with the first three branches of the L mode are shown in Fig. 3, and we see that they must be reidentified as follows: his branch one results belong to L^1 for $ka < \pi/2$ and to S_1^1 for $ka > \pi/2$; his branch two results belong to S_1^1 for $ka < \pi/2$ and to L^1 for $ka > \pi/2$; his third branch is actually the branch S_1^2. Nigro's reidentified results are in excellent agreement with the present results.

Also shown in Fig. 3 is the fundamental branch of the dispersion curves for longitudinal waves in a circular bar with the same area as the square bar. This curve is very close to the L^1 branch for the square bar, in agreement with the experimental results of Morse [3] for brass bars.

Figure 4 shows the change in the distribution of u_z and σ_{zz} on the x (or y) axis of the square bar cross-section as ka increases along the L^1 branch. When $ka = 1$, u_z and σ_{zz} are maximum on the axis of the bar and decrease slightly towards the boundary. As ka increases from 2 to 5 the distributions become zero (at approximately $ka = 2 \cdot 4$) and then negative at the boundary (taking u_z and σ_{zz} positive on the z-axis). As ka continues to increase u_z and σ_{zz} become very small at the z-axis, increase to a positive maximum near the boundary and then fall rapidly through zero to become large and negative on the boundary. For $ka = 16$ the distributions resemble those for Rayleigh waves on the surface of an elastic half-space (cf. Kolsky [11]).

(ii) *Rectangular bars.* Lamé waves propagate in all bars of width $2a$ with wave numbers given by $ka = n\pi/2$ (n odd) independently of the depth $2b$, and the dispersion curves for longitudinal waves in bars of equal width but different depths have common points. For each bar there will also be Lamé waves associated with the depth which have frequencies given by $kb = n\pi/2$ (i.e. $ka = an\pi/2b$), n odd.

Figure 5 shows the first two branches of the dispersion curves for longitudinal waves in various rectangular bars of equal width and $b/a > 1$. The Lamé wave of lowest frequency is the one for which $ka = a\pi/2b$, and this point lies on the L^1 branch for each bar. As b/a increases these branches are displaced further to the left in Fig. 5. The lowest frequency Lamé wave associated with the width is the one for which $ka = \pi/2$, and this is the common point of the second branches provided $b/a \leq 3$. If $3 < b/a < 5$ the second Lamé wave associated with the depth has a frequency given by $ka = 3a\pi/2b < \pi/2$. For such a bar it seems reasonable to assume that the second branch will pass through this point and that the third or higher order branch will pass through the common point $ka = \pi/2$.
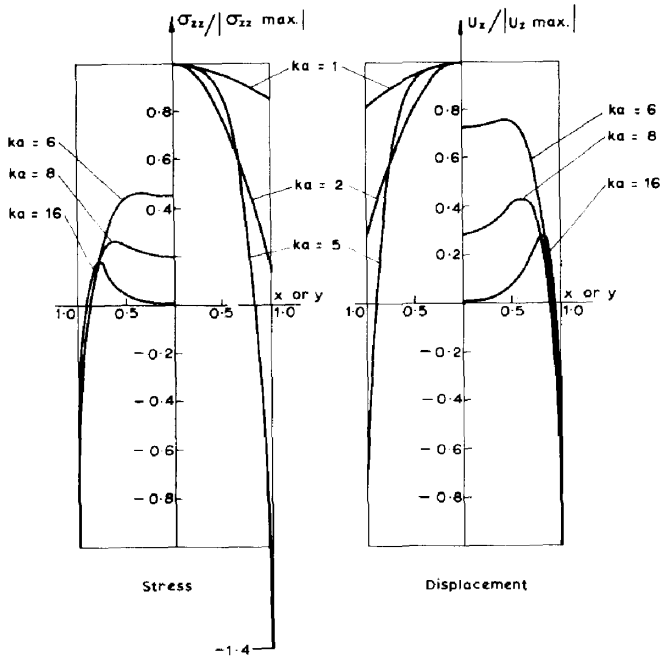
Poisson's ratio 0·3

FIG. 4. Distribution of normal stress and displacement on the x (or y) axis of the square bar cross-section for values of ka on branch L^1.
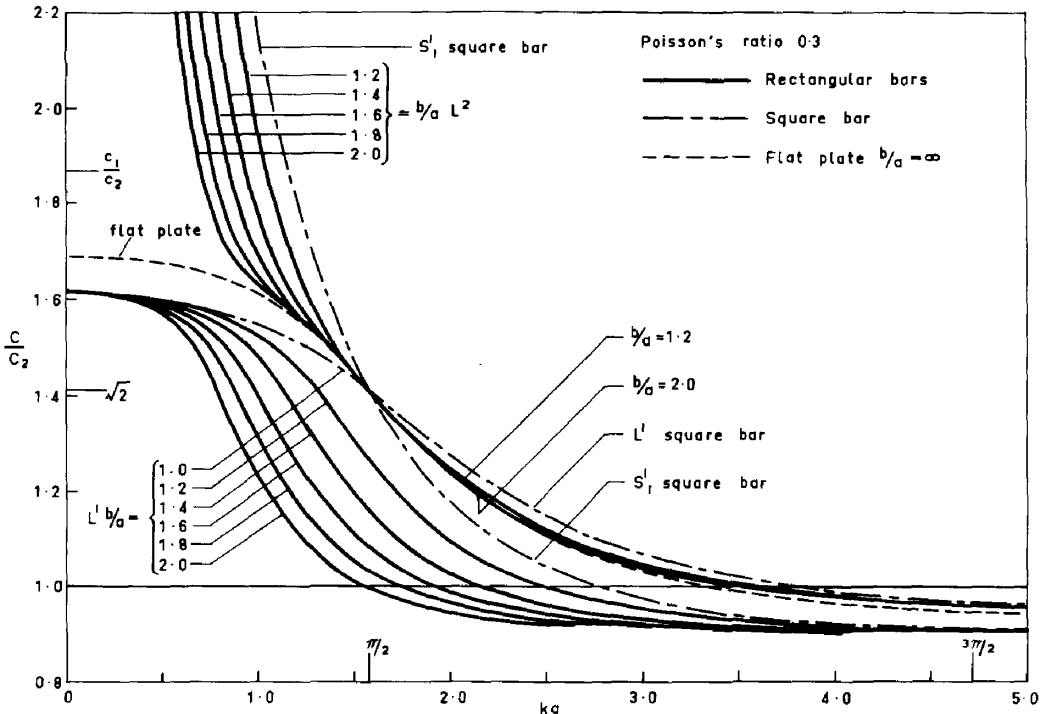

FIG. 5. Dispersion curves for rectangular bars: branches L^1 and L^2, with square bar and flat plate results.

(Note that there may be other branches between those identified with the Lamé waves.) As b/a increases more and more branches will lie between the fundamental and the branch through the point $ka = \pi/2$, $c/c_2 = \sqrt{2}$. Because of the limitations of the collocation method the largest value of b/a investigated was $b/a = 2$. However, in the limit $b/a = \infty$ we have an infinite flat plate of thickness $2a$ which can be treated analytically. (See for example Morse [3].) The fundamental dispersion curve for symmetrical (longitudinal) waves in a plate is also shown in Fig. 5, and it is interesting that although this curve does not exhibit cut-off it is grouped with the L^2 branches of the bars treated here.

Of course, if $b/a < 1$ the above situation is reversed, the first branches have a common point at $ka = \pi/2$, and the second branches are displaced to the right with decreasing depth. Results for this case could be obtained from the present results by plotting kb on the abscissa instead of ka.

Morse [3] obtained the first two branches for longitudinal modes in rectangular brass bars, of equal widths $2a$ but various depths ($b > a$), experimentally. His results show all the features shown in Fig. 5 (except for the screw mode branch S_1^1 for the square bar).

We have already shown that the longitudinal and first screw modes which are distinct in a square bar couple to give only a longitudinal mode in a rectangular bar. We investigate this coupling in a rectangular bar for which $b/a = 1.2$. Notice in Fig. 5 that the L^1 branch for this one bar, lies close to the L^1 branch for the square bar for small values of ka, while for large values of ka it lies close to the S_1^1 branch for the square bar. The opposite is true of the L^2 branch. Kynch [2] also found this to be so, and showed that waves in a rectangular bar corresponding to points on the L^1 branch are predominantly of longitudinal type at low frequencies ($ka < \pi/2$) and predominantly of screw type at high frequencies ($ka > \pi/2$), the reverse being true for the second branch. Figure 6 shows the displacement of the boun-

L^1: $ka = 1.0$, $\frac{c}{c_2} = 1.529$ L^1: $ka = 6.0$, $\frac{c}{c_2} = 0.904$

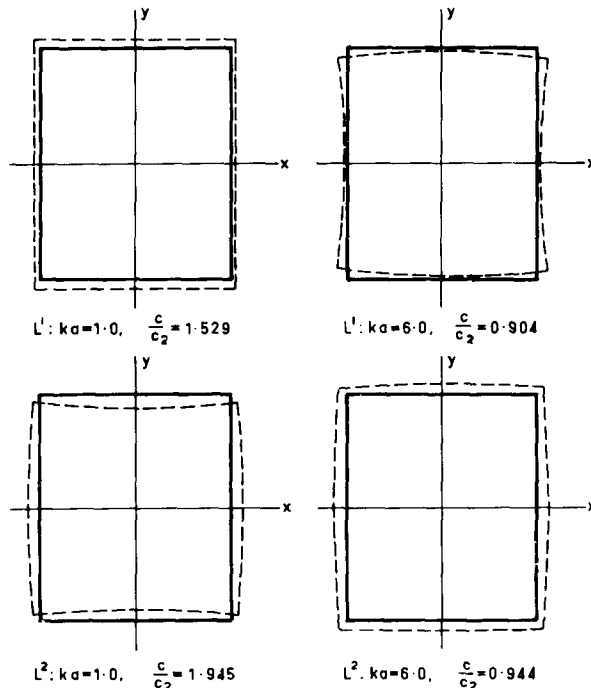L^2: $ka = 1.0$, $\frac{c}{c_2} = 1.945$ L^2: $ka = 6.0$, $\frac{c}{c_2} = 0.944$

FIG. 6. Distortion of the boundary of the rectangular cross-section $b/a = 1.2$.

dary of the rectangular cross-section for waves corresponding to points on the L^1 and L^2 branches for two values of ka. For $ka = 1$ the L^1 branch wave produces a dilatational distortion of the boundary, whereas the L^2 branch wave produces the screw type distortion of the boundary. For $ka = 6$ the L^1 branch wave produces the screw type distortion and the L^2 branch wave produces the dilatational distortion.

(b) *Torsional and second screw modes*

Figure 7 shows the T^1 and S_2^1 branches for a square bar and the T^1 and T^2 branches for the rectangular bar for which $b/a = 1.2$. The T^1 branches lie close together as do the
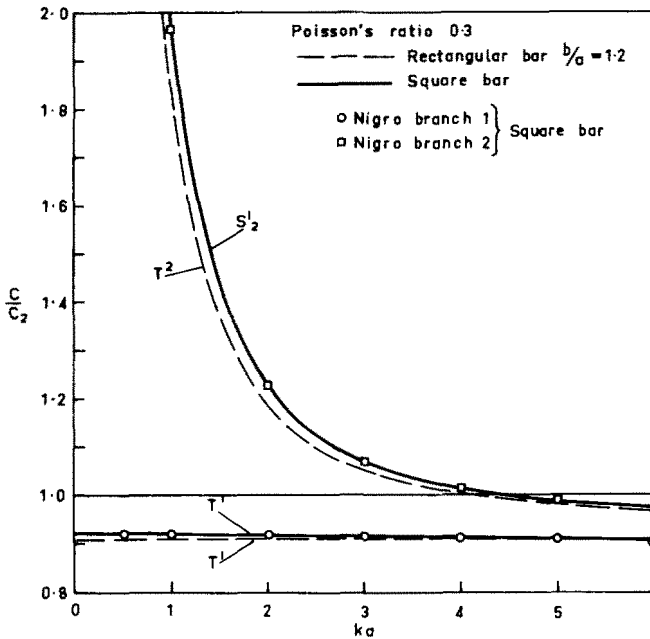

Fig. 7. Dispersion curves for a rectangular bar: branches T^1 and T^2, and a square bar: branches T^1 and S_2^1.

T^2 and S_2^1 branches, and the effect of the coupling of the screw with the torsional mode in the rectangular bar is seen to be slight compared with the corresponding effect for the longitudinal and first screw modes. Nigro's results for the first two torsional mode branches for a square bar are also shown, and we see that his second branch is actually the screw mode branch S_2^1. The agreement with Nigro's reidentified results is good, although his T^1 branch has a minimum at $ka = 8$ (approximately) which is not found in the present results (see Table 1) where c/c_2 decreases monotonically out as far as $ka = 14$.

(c) *Bending modes*

Figure 8 shows the first two branches for bending waves in a square bar and the rectangular bar for which $b/a = 1.2$. Nigro's results for the square bar are also shown, and again the agreement with them is excellent.
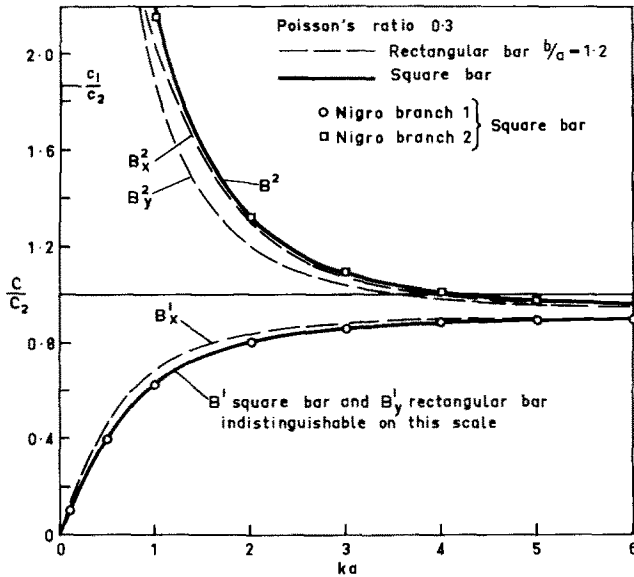
FIG. 8. Dispersion curves for bending waves in a square and a rectangular bar.

6. COMPARISON WITH APPROXIMATE THEORIES

One of the purposes of seeking solutions of the exact equations of motion for elastic bars by numerical methods, is to aid in assessing the accuracy of results obtained from various approximate theories. Here we confine our attention to an assessment of two recent theories due to Volterra [12] and Medick [13, 14] by comparing longitudinal wave dispersion curves obtained using these theories with those obtained using the collocation method. Earlier approximate theories have been discussed in detail in the review paper by Green [1].

Volterra and Medick both use approximate displacement functions in conjunction with Hamilton's principle to satisfy the field equations and boundary conditions approximately. Volterra uses simple power series in the lateral coordinates x and y to represent displacements, whereas Medick uses a suitably truncated series in products of Legendre polynomials in x and y. Both theories lead eventually to third order characteristic determinants that give the dispersion relations for longitudinal waves. Medick's $(1, 1)$ theory, appropriate for bars where b/a is near one, leads to a characteristic determinant (equation (56) of reference [13]) which in the notation of this paper is

$$
\begin{vmatrix}
\left[\left(\dfrac{c_1}{c_2}\right)^2 - \left(\dfrac{c}{c_2}\right)^2\right]\left[\left(\dfrac{c_1}{c_2}\right)^2 - 2\right] & \left[\left(\dfrac{c_1}{c_2}\right)^2 - 2\right] \\[4mm]
\left[\left(\dfrac{c_1}{c_2}\right)^2 - 2\right] & \left\{\left(\dfrac{2\alpha ka}{\pi}\right)^2\left[1 - \left(\dfrac{c}{c_2}\right)^2\right] + \left(\dfrac{c_1}{c_2}\right)^2\right\} \quad \left[\left(\dfrac{c_1}{c_2}\right)^2 - 2\right] \\[4mm]
\left[\left(\dfrac{c_1}{c_2}\right)^2 - 2\right] & \left[\left(\dfrac{c_1}{c_2}\right)^2 - 2\right] \qquad\qquad \left\{\left(\dfrac{2\alpha ka}{\pi}\right)^2\left(\dfrac{b}{a}\right)^2\left[1 - \left(\dfrac{c}{c_2}\right)^2\right] + \left(\dfrac{c_1}{c_2}\right)^2\right\}
\end{vmatrix} = 0.
$$

Volterra's dispersion relation for longitudinal waves (equation (61) of reference [12]) in determinental form is obtained from (7) by replacing the diagonal terms D_{ii} by

$$
\left.
\begin{aligned}
D_{11} &= 3\left[\left(\frac{c_1}{c_2}\right)^2\left(1 - \frac{4}{3}\frac{v^2}{1-v}\right) - \left(\frac{c}{c_2}\right)^2\right], \\
D_{22} &= (ka)^2\left[K - \left(\frac{c}{c_2}\right)^2\right] + \left(\frac{c_1}{c_2}\right)^2, \\
D_{33} &= (ka)^2\left(\frac{b}{a}\right)^2\left[K - \left(\frac{c}{c_2}\right)^2\right] + \left(\frac{c_1}{c_2}\right)^2.
\end{aligned}
\right\}
\tag{8}
$$

The factors α and K that appear in (7) and (8) are adjustment parameters introduced into the strain energy integral in Hamilton's principle to partially compensate for the restricted dependence of the strain variables on the lateral coordinates x and y (cf. equation (8) of reference [12] and equation (44) of reference [13]). Medick sets $\alpha = 1$ so that "the predictions of the (1, 1) theory coincide with those of the analogous plate theory for degenerate cross-sections, i.e. the infinite plate and the narrow strip". [13]. We see from (7) that the limiting phase velocities for very small or very large wave numbers are independent of α and have the values, for the three branches of the dispersion curves defined by (7), of

$$c = c_0, \infty, \infty, \quad \text{for} \quad ka \ll 1,$$

$$c = c_2, c_2, c_1, \quad \text{for} \quad ka \gg 1,$$

where c_0 is the bar velocity.

Volterra sets the factor $K = (c_s/c_2)^2$, where c_s is the Rayleigh surface wave velocity [11]. With this choice of K the limiting values of phase velocity for large wave numbers are

$$c = c_s, c_s, c_1; \quad ka \gg 1,$$

and for small wave numbers the limiting value of phase velocity is independent of K:

$$c = c_0, \infty, \infty; \quad ka \ll 1.$$

Figure 9 shows the lowest two branches of the dispersion curves for a square bar calculated from the Medick and Volterra determinants (for $v = 0{\cdot}3$, $\alpha = 1$ and $K = 0{\cdot}8601$) compared with branches L^1 and S_1^1 obtained by the collocation method. Branches L^1 and S_1^1 obtained from Medick's determinant intersect at the correct phase velocity ($c = c_2\sqrt{2}$) but the corresponding value of $ka = \pi/\sqrt{2}$ is too large, and of course the asymptotic value of phase velocity is c_2 rather than c_s. Branch L^1 obtained from the Volterra determinant is in better agreement with the collocation result but the S_1^1 branch is not, and their intersection is in error in both coordinates. The reason Volterra's L^1 branch is a better fit than Medick's is probably because his polynomial approximation to the displacement is of a higher degree than that of Medick's truncated Legendre polynomial in his (1, 1) theory.

The accuracy of the dispersion curves obtained from Medick's determinant can be considerably improved by choosing α to make the Lamé wave roots ($c/c_2 = \sqrt{2}$; ka, $kb = \pi/2$) satisfy the determinant. This is accomplished by setting $\alpha = \sqrt{2}$. Figure 10 shows the results with this choice of α for bars for which $b/a = 1{\cdot}0$, $1{\cdot}4$ and $1{\cdot}8$, plotted with the corresponding results obtained by the collocation method.
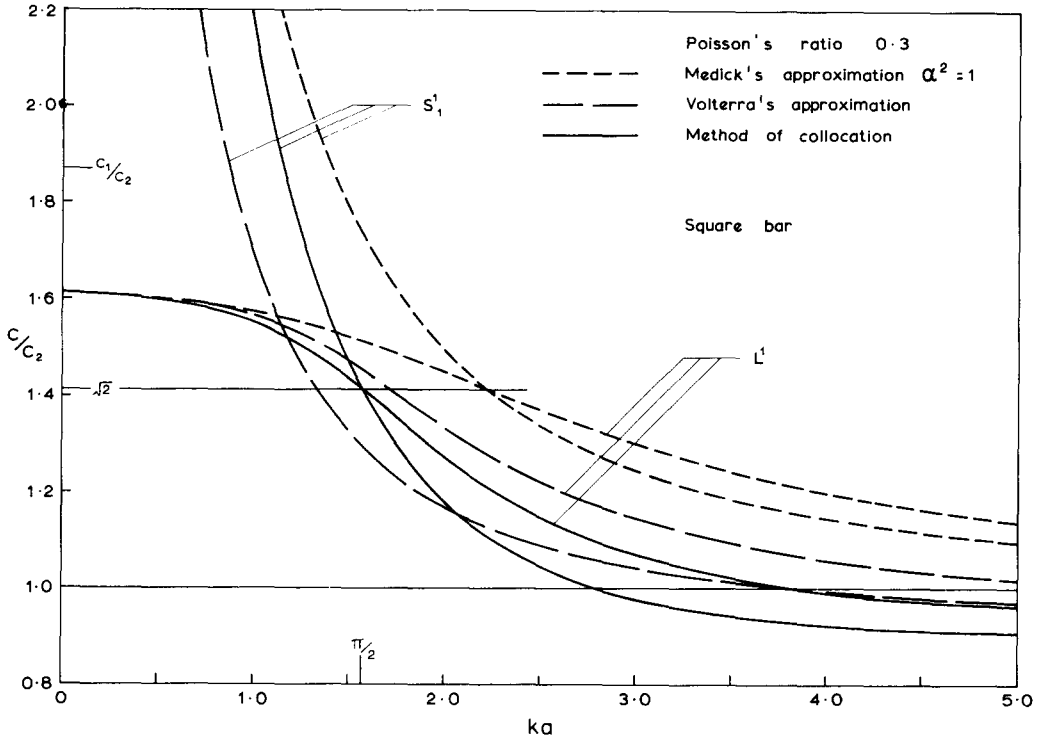
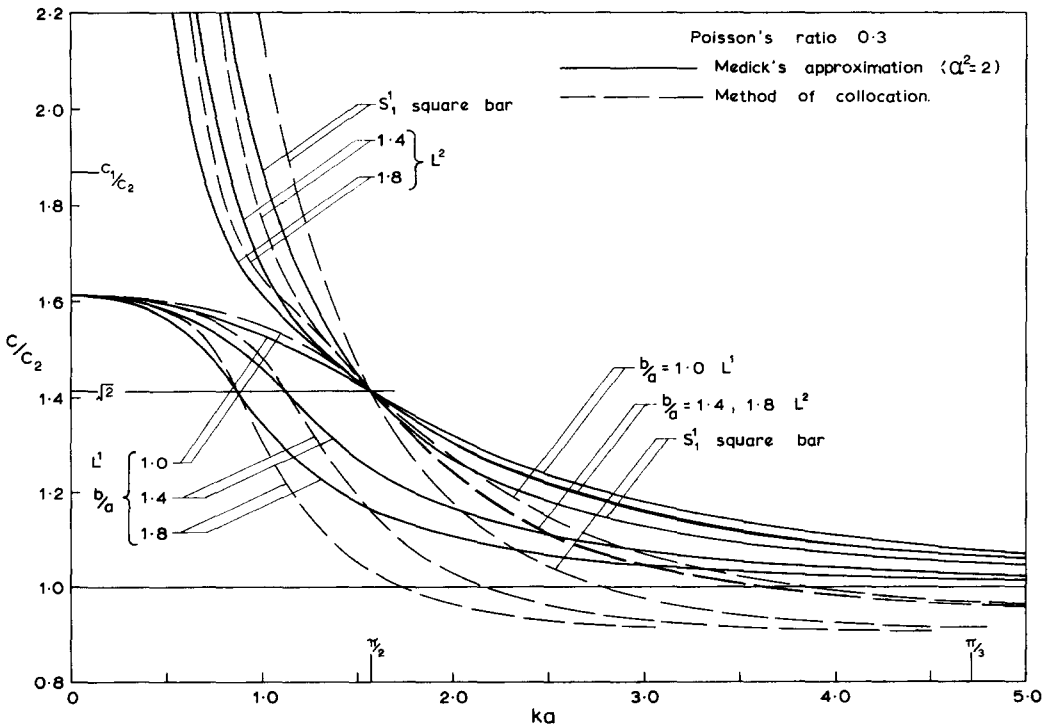FIG. 9. Approximate theory dispersion curves for a square bar: branches L^1 and S_1^1.

FIG. 10. Approximate theory dispersion curves for rectangular bars: branches L^1 and L^2.

Of course both approximate theories give dispersion curves that have the correct general form, and because of the comparative simplicity of the dispersion relations they are useful for making qualitative predictions of the effects of dispersion in rectangular bars even if the quantitative results are in error.

REFERENCES

[1] W. A. GREEN, *Progress in Solid Mechanics*, Vol. 1, pp. 225–261. North-Holland (1960).
[2] G. J. KYNCH, The fundamental modes of vibration of uniform beams for medium wavelengths. *Br. J. appl. Phys.* **8**, 64–73 (1957).
[3] R. W. MORSE, Dispersion of compressional waves in isotropic rods of rectangular cross section. *J. acoust. Soc. Am.* **20**, 833–838 (1948).
[4] N. J. NIGRO, Steady-state wave propagation in infinite bars of noncircular cross section. *J. acoust. Soc. Am.* **40**, 1501–1508 (1966).
[5] L. FOX, P. HENRICI, and C. MOLER, Approximations and bounds for eigenvalues of elliptic operators. *SIAM J. numer. Anal.* **4**, 89–102 (1967).
[6] H. D. CONWAY and A. W. LEISSA, A method for investigating certain eigenvalue problems of the buckling and vibration of plates. *J. appl. Mech.* **27**, 557–558 (1960).
[7] H. D. CONWAY and K. A. FARNHAM, The free flexural vibrations of triangular, rhombic and parallelogram plates and some analogies. *Int. J. mech. Sci.* **7**, 811–816 (1965).
[8] G. J. KYNCH and W. A. GREEN, Vibrations of beams. I: Longitudinal modes. *Q. Jl Mech. appl. Math.* **10**, 63–73 (1957).
[9] G. LAMÉ, *Leçons sur la Théorie Mathématique de l'elasticité des Corps Solides*, p. 170. 2nd edition. Gauthier-Villars (1866).
[10] R. D. MINDLIN and E. A. FOX, Vibration and waves in elastic bars of rectangular cross-section. *J. appl. Mech.* **27**, 152–158 (1960).
[11] H. KOLSKY, *Stress Waves in Solids*, p. 22. Dover (1963).
[12] E. VOLTERRA, Second approximation of method of internal constraints and its applications. *Int. J. mech. Sci.* **3**, 47–67 (1961).
[13] M. A. MEDICK, One-dimensional theories of wave propagation and vibrations in elastic bars of rectangular cross-section. *J. appl. Mech.* **33**, 489–495 (1966).
[14] M. A. MEDICK, On the dispersion of longitudinal waves in rectangular bars. *J. appl. Mech.* **34**, 714–717 (1967).

Абстракт—Используется метод коллокации цля определения кривых дисперсии при распределении волн в бесконечных прямоугольных стержнях. Получаются тщательные результаты, сверх ограниченого предела числа волн, для первых двух ветвей кривых дисперсии для разных видов распределения. Определяются винтовые виды Кинча для квадратного стержня. Исследуется, подробно, взаимодействие между одним из винтовых видов и продольной формой. Наконец, эти результаты используются для оценки тщательности двух, выведенных в последнее время, приближвнных теорий волн.